Scientia Iranica B (2015) 22(3), 765–777

Sharif University of Technology
Scientia Iranica
Transactions B: Mechanical Engineering
www.scientiairanica.com

Rooster tail depression by originating a modified transom stern form using a Reynolds averaged Navier Stokes solver

P. Ghadimi*, A. Dashtimanesh, R. Zamanian, M.A. Feizi Chekab and S.H.R. Mirhosseini

Department of Marine Technology, Amirkabir University of Technology, Teheran, Iran.

Received 2 November 2012; received in revised form 12 September 2014; accepted 29 November 2014

KEYWORDS
Hydrodynamics;
Transom cut;
Rooster tail reduction;
Numerical simulation;
Parametric study.

Abstract. The present article relates to a new transom stern form for high speed planing hulls. To depress the intensive transom wave known as a "rooster tail", an innovative form of transom stern is originated. The new form of the transom stern is introduced by cutting the bottom of the hull near the transom stern. To verify the capability of the modified transom stern, a three dimensional RANS solver is used. It is demonstrated that by using the new transom stern shape, the intensive wave behind the transom will be substantially reduced in the range of the parameters under investigation. In the meantime, it is expected that the radar signature will also be decreased.

To study the effect of the modified transom at various Froude numbers and different trim angles, a set of numerical experiments are conducted. Three Froude numbers and four trim angles are considered and it is observed that the cutted transom stern has a significant effect on the reduction of height and length (height reduction up to 61% and length reduction up to 63%) of the rooster tail. Additionally, the accuracy of the numerical solutions is validated by comparing them against the results of empirical formula existing in the literature.

1. Introduction

It is well known that using the transom stern on the planing hull leads to an intensive wave known as a "rooster tail". Although, the truncated shape of stern will amount to some benefits, generated rooster tail brings about the strength of radar signature. However, the reduction of rigorous transom wave may cause a decrease in the radar's signals. As important as this topic is, only a few authors have tried to reduce the rooster tail.

Karafiath and Fisher [1] investigated the effect of stern wedge on the powering performance and annual fuel consumption of a destroyer and a frigate size ship. They claimed that the wedge significantly decreases the stern wave height. It is also shown that the wedge significantly affects the flow velocity near the afterbody. Cusanelli and O'Connell [2] performed model experiments in 1999 to evaluate the performance of a stern flap on a patrol boat. They also declared that the transom flow appears to decrease in both wave height and overall width by the stern flap, in a special speed range.

In 2001, Karafiath et al. [3] designed a stern flap, spray rail and a new propeller for hydrodynamic improvement of patrol boats. By using the stern flap, the transom wave was decreased in a specific speed range. The effects of stern flaps on the hydrodynamic

*. *Corresponding author. Tel.: +98 21 64543120; Fax: +98 21 66412495*
E-mail address: pghadimi@aut.ac.ir (P. Ghadimi)

performance of a semi displacement hull were evaluated by Salas et al. [4]. They found that a stern flap can affect the stern zone flow by reducing the height, slope, wave breaking and amount of white water in the trailing waves. Model experiments have shown a reduction of wave heights in the near field stern wave. Yamano et al. [5,6] in two separate works tried to design a waveless transom stern wave. The stern wave has been modified by bottom slope variations.

Recently, Ogilat et al. [7] considered the free surface flow past a two-dimensional semi-infinite curved plate. Different shapes of the semi-infinite plate were examined and it was shown how the amplitude of the waves can be minimized.

As mentioned before, rooster tail reduction has only been considered by few authors. However, the phenomena related to transom stern flow has been considered by many authors numerically as well as experimentally. Continuing with the literature study, major experimental and numerical works related to transom stern will be reviewed.

A set of experiments was carried out by Robards and Doctors [8] on the rectangular transom stern to survey transom ventilation as well as longitudinal wake profile. The process of transom stern ventilation at low speed was also considered by Doctors [9,10] and empirical formulas have been derived.

Some interesting results were achieved by Maki et al. [11], and complete descriptions of the nature of the transom stern ventilation were presented in their study in 2005. Doctors and Beck [12] explored the geometry of transom hollow in many different conditions by measuring the transom flow and, so, new regression formulas were developed. Two series of experiments on the destroyer vessels were conducted by Maki et al. [13] to analyze the transom stern flow of a high speed craft.

Recently, in 2009 and 2010, Fu et al. [14,15] prepared an experimental setup for detailed measurement of the turbulent multiphase flow associated with transom wave breaking. Measurement system was capable of high sampling rate and large dynamic ranges. Sinkage and trim, drag, vertical and side force as well as spray and free surface deformation were quantified in their study. For the first time in 2009, Savitsky and Morabito [16] considered a set of experiment on the planing hulls. Three prismatic planing hulls with deadrise angles 10, 20 and 30 degrees were investigated at different positions. Some empirical relations based on the experimental data have been developed. In the present study, these relations are utilized to validate our numerical model of the transom stern flow.

In addition to the mentioned experimental studies, some researchers have also tried to present numerical solutions. Haussling [17] presented a two dimensional boundary element solution to simulate linear and nonlinear fluid flows behind a semi-infinite body. A three dimensional transom stern flow was considered by Cheng [18] in 1989. He used the Rankine Panel method with linear free surface condition to probe the transom stern ventilation. Scorpio and Beck [19], using boundary element method, presented a two dimensional nonlinear transom stern solution. It was shown that the pressure reduction can lead to flow separation from transom. Effects of transom stern on the resistance of high speed craft, using panel method, was investigated by Sireli et al. [20]. In 2010, Binder [21] presented a new boundary integral solution for the free surface flow passing a curved plate in correspondence with the transom stern flow.

Haussling et al. [22] used the RANS solver to study the steady fluid flow around the transom stern of a displacement vessel. Transom waves were numerically studied by Schweighofer [23]. He also used the RANS method and FINFLO solver to model the two dimensional transom stern wave. Starke et al. [24] performed a computational study using RANS method and PARNASOS solver. Different aspects of transom waves were surveyed in his study.

In recent years, the studies of Maki et al. [25] and Maki [26] gave a comprehensive understanding of the transom stern flow phenomenon. Numerical computations using a level set method code and the Volume of Fluid method using Fluent, and implementation of two turbulent models were the main characteristics of these studies.

From the presented literature review, it can be concluded that one of the main computational challenge in the transom stern field is the three dimensional viscous solution of free surface flow which is considered in the present study. A new and distinctive shape of the transom stern which reduces the rooster tail is also introduced, and extensive parametric studies are performed at different speeds and trim angles.

In general, three important features which can be considered as main novelties of the present article can be categorized as follows:

- Three dimensional viscous numerical solution of transom stern flow using FVM/VOF in Ansys-CFX software;
- Offering an innovative form of the transom stern;
- Performing extensive set of parametric studies at different Froude numbers and trim angles, numerically;
- New physical findings.

In the following sections, after describing the setup of the investigation, the governing equations and the required boundary conditions are discussed. Also, a mesh convergence study is undertaken in Section 4 to obtain an optimal mesh size after which the validation of the numerical model is presented in Section 5 by the

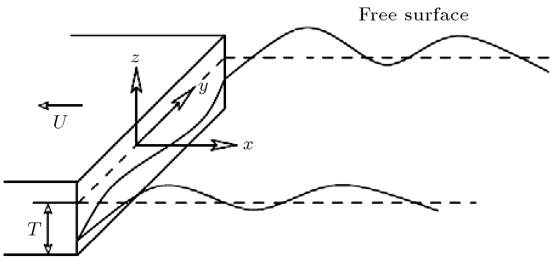

Figure 1. Prismatic hull with free surface configuration.

use of experimental data of Savitsky and Morabito [16] for studying the rooster tail of a planning hull. Afterward, a parametric study of the trims and Froude numbers for the proposed innovative stern is presented in Section 6 followed by the conclusion in Section 7.

2. Problem definition

Figure 1 shows a prismatic planing hull which is moving in a free surface with velocity U. It has a deadrise angle β, trim angle τ and a draught T. A coordinate system (x, y, z) is also depicted in Figure 1 whose origin is at the intersection of the transom stern and the undisturbed free surface. The rooster tail just behind the transom stern is the focus of the present article.

Furthermore, in the present study, the length Froude number is considered as a main non-dimensional parameter. The length Froude number is defined as $F_L = U/\sqrt{gL}$ in which L denotes the hull length. Different trim angles and various lengths Froude numbers are investigated and a specific draught is used.

3. Reduction scheme

Reduction of transom stern wave leads to the reduction of the radar signature as well as minimization of the fuel consumption. When the rooster tail that has its crest in the center plane is reduced, the whole wake of the transom stern is decreased and consequently, the fuel consumption of the hull is decreased proportionally, as the wave making of the hull is decreased. In the present article, an innovative shape of the transom stern is introduced which modifies the flow of water underneath and around it, in a way that the rooster tail at different speeds is significantly reduced.

The suggested transom shape is illustrated in Figure 2. It modifies the strong pressure variation in the transom stern and leads to rooster tail reduction which will be shown in the next sections. To verify the performance of the new transom stern, the Ansys-CFX RANS solver is utilized in three dimensions and an extensive set of parametric studies is conducted.

It should be noted that the angle o, the cut length L_C and H_C are the main parameters that determine the dimensions of the cut, as shown in Figure 2.

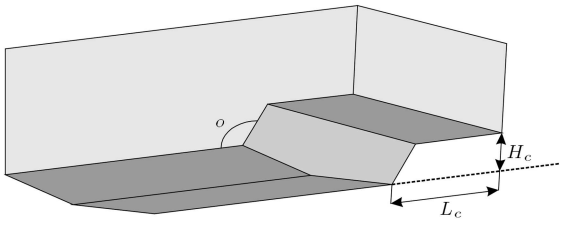

Figure 2. New transom stern form.

4. Numerical solution

Navier-Stokes equations accurately describe fluid flow for a remarkably large class of problems. When Navier-Stokes equations are decomposed into the RANS (Reynolds Averaged Navier-Stokes) equations, simulation of fluid flow phenomenon such as transom stern flow will become possible. In the Ansys-CFX, the RANS equations are combined with some practical assumptions. These assumptions lead to simple solution of large variety of fluid flow problems within Ansys-CFX.

The assumption behind the RANS equations is that the time-dependent turbulent velocity fluctuations can be separated from the mean flow velocity. Therefore, Reynolds stresses which are generally unknown will be introduced. Implementing a turbulence model such as K-Epsilon is also necessary because velocity fluctuations have strong effects on Reynolds stresses. Finally, an algebraic system of equations will be generated.

The fluid flow governing equations in conjunction with turbulent model, boundary conditions, mesh convergence study and validation of the three dimensional numerical model will be presented in the following subsections.

4.1. Governing equations

The fundamental basis of fluid dynamics is the Navier-Stokes equations. The incompressible form of these equations and the incompressible continuity equation are described as bellow [27].

$$\frac{\partial u_i}{\partial t} + u_j \frac{\partial u_i}{\partial x_j} = -\frac{1}{\rho}\frac{\partial p}{\partial x_i} + \frac{\partial}{\partial x_j}\left(\frac{\mu}{\rho}\frac{\partial u_i}{\partial x_j}\right), \tag{1}$$

$$\frac{\partial u_i}{\partial x_i} = 0, \tag{2}$$

where x_i ($i = 1, 2, 3$) are the Cartesian coordinates, (x, y, z), u_i are the Cartesian components of the velocity, t is the time, p is the pressure, ρ is the density and μ is the dynamic viscosity, defined as the viscosity μ divided by ρ.

In the RANS approach to turbulence, all of the unsteadiness in the flow is averaged out and regarded as part of the turbulence. The flow variables, in this example one component of the velocity, are represented

as the sum of two terms [28] as in:

$$u_i(x_k,t) = U_i(x_k) + u'_i(x_k,t), \tag{3}$$

where:

$$U_i(x_k) = \lim_{T\to\infty} \frac{1}{T}\int_0^T u_i(x_k,t)\,dt.$$

Here, T is the averaging interval and must be large compared to the typical time scale of the fluctuations and u'_i is the fluctuation about the time averaged value. Finally, substituting Eq. (3) into Eqs. (1) and (2) (and averaging) yields in:

$$\frac{\partial U_i}{\partial t} + U_j\frac{\partial U_i}{\partial x_j} = -\frac{1}{\rho}\frac{\partial p}{\partial x_i} + \frac{\partial}{\partial x_j}\left(\frac{\mu}{\rho}\frac{\partial U_i}{\partial x_j}\right) + \frac{\partial(-\bar{u}'_i\bar{u}'_j)}{\partial x_j},$$

$$\frac{\partial U_i}{\partial x_i} = 0. \tag{4}$$

To consider the Reynolds stress term, $\bar{u}'_i\bar{u}'_j$, a two equation k-ε model is utilized. The exact equations for the k and ε parameters are as follows:

$$\frac{\partial k}{\partial t} + U_j\frac{\partial k}{\partial x_j} = \frac{\mu_t}{\rho}S^2 - \varepsilon + \frac{\partial}{\partial x_j}\left[\frac{1}{\rho}\left(\mu + \frac{\mu_t}{\sigma_k}\right)\frac{\partial k}{\partial x_j}\right], \tag{5}$$

$$\frac{\partial \varepsilon}{\partial t} + U_j\frac{\partial \varepsilon}{\partial x_j} = \frac{\varepsilon}{k}\left(C_{1\varepsilon}\frac{\mu_t}{\rho}S^2 - C_{2\varepsilon}\varepsilon\right) + \frac{\partial}{\partial x_j}\left[\frac{1}{\rho}\left(\mu + \frac{\mu_t}{\sigma_\varepsilon}\right)\frac{\partial \varepsilon}{\partial x_j}\right], \tag{6}$$

where k is the turbulent kinetic energy and ε is the dissipation rate of the turbulence energy. Parameters σ_k, σ_ε, $C_{1\varepsilon}$, $C_{2\varepsilon}$, C_μ are five free constants. Also, μ_t is the turbulent eddy viscosity and $\frac{\mu_t}{\rho}S^2$ is the turbulence production due to the viscous force.

Furthermore, to capture the sharp interface in hydrodynamics of two-phase flow problems, a Volume Of Fluid method (VOF) is employed. The VOF technique uses a color function named Volume Fraction (α). A transport equation (Eq. (7)) is then solved for the advection of this scalar using the velocity field calculated from the solution of the Navier-Stokes equations at the last time step:

$$\frac{\partial x}{\partial t} + u_j\frac{\partial x}{\partial x_j} = 0. \tag{7}$$

Numerical solution of Eq. (7) gives the volume fraction of each phase (i.e. air and water) in all computational cells. Distribution of the volume fraction (α) is as follows:

$$\alpha = \begin{cases} 1 & \text{for cells including fluid 1} \\ 0 & \text{for cells including fluid 2} \\ 0<\alpha<1 & \text{for cells including the interface} \end{cases} \tag{8}$$

Using the volume fraction, an effective fluid with variable physical properties is introduced:

$$\rho_{\text{eff}} = \alpha\rho_1 + (1-\alpha)\rho_2,$$

$$\upsilon_{\text{eff}} = \alpha\upsilon_1 + (1-\alpha)\upsilon_2, \tag{9}$$

where subscripts 1 and 2 represent two phases, i.e. water and air. As pointed out earlier, governing equations are solved using the combination of Finite Volume and Volume of Fluid methods by the Ansys-CFX solver.

4.2. Boundary conditions

When simulating the free surface flows, appropriate initial conditions and boundary conditions must be defined to set up appropriate velocity and volume fraction fields. It is necessary to create expressions using CEL (CFX Expression Language) to define these conditions. In the present article, the following conditions are set:

1. An inlet boundary where the volume fraction above the free surface is 1 for air and 0 for water and below the free surface is 0 for air and 1 for water. It must be noted that placing a velocity inlet too close to a solid obstruction must be avoided. This can force the solution to be non-physical.
2. A pressure specified outlet boundary, where the pressure above the free surface is constant and the pressure below the free surface is a hydrostatic distribution.
3. The bottom, top and side (opposite the symmetry plane on centerline) faces are velocity inlets.
4. A no-slip boundary condition is also applied on the body.

As declared in the above paragraphs, all the faces, with the exception of the outlet, are considered as inlet boundary condition. In fact, by choosing the inlet boundary condition, the rate of convergence increases and the computational time will be reduced.

It is also noteworthy that a length scale of 3.5 m and a Fractional Intensity of 5% has been used for the turbulence inlet boundary condition.

4.3. Mesh convergence study

The computational domain is meshed by using the CFX mesh generator and tetrahedral grid elements are also utilized. It must be noted that using refined mesh over the transom stern region is vital to get a sharp free surface. The point controls feature is also utilized to control the mesh based on a sphere of influence

Table 1. Mesh convergence study.

Case	Element size (m)	No. of mesh elements
1	0.03529	9009130
2	0.03555	7995352
3	0.039998	7002432
4	0.041222	6163243
5	0.0442	5002155
6	0.04955	3996824
7	0.05888	3000337
8	0.06932	2000511
9	0.1138	1000156

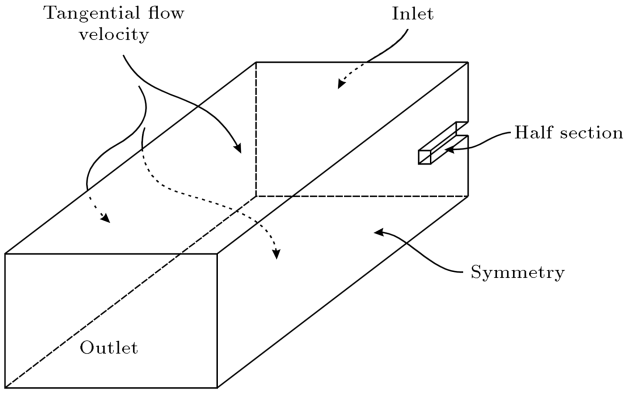

Figure 3. Computational domain and boundary conditions.

technique. In fact, the sphere of influence technique is implemented in order to perform mesh refinement along the free surface just behind the transom stern.

In the numerical computations, a finer mesh usually results in a more accurate solution. However, as mesh gets finer, the computation time increases. Therefore, we must obtain a mesh that satisfactorily balances accuracy and computing resources. For this purpose, several grid sizes which are presented in Table 1 are considered. Main attention must also be paid to the sensitivity of the rooster tails to mesh refinement.

Resulted rooster tails at various element sizes are represented in Figure 3. The element size is defined as the length of elements edge in the modeled hull which is measured in meters.

The resulting rooster tail free surfaces for different mesh sizes are plotted in Figure 4.

Based on Figure 4, it can be concluded that the free surface profiles are similar when the number of elements considered is more than seven million.

5. Validation

After performing the mesh optimization study, the validity of numerical computation must be proved.

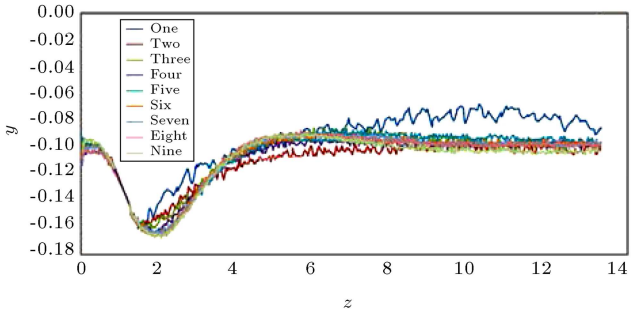

Figure 4. Free surface profiles for different grid numbers.

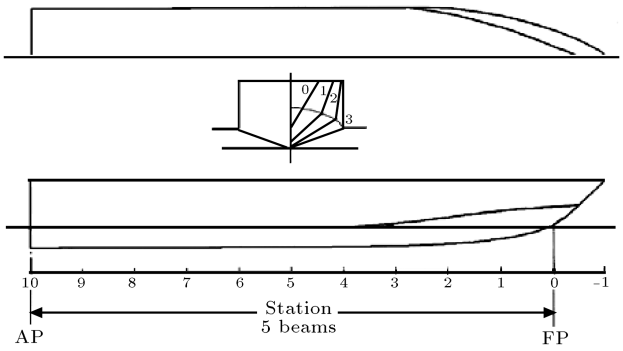

Figure 5. Prismatic planning hull [16].

Savitsky and Morabito [16] obtained some empirical formulas based on their experimental study. These empirical formulas are used to evaluate the accuracy of the presented numerical simulation. It must be emphasized that these formulas can only be used in the specific range of Froude number, trim angle and deadrise angle [16].

Here, a prismatic planing hull which is shown in Figure 5 is considered. This hull was implemented in the experimental studies of Savitsky and Morabito [16]. The hull length (L) is equal to 1.22 m while the width (B) is 3.0 cm. The deadrise angle of the planning hull is also 20 degrees. The dimensions of the computational domain extend out for approximately $15L$ behind the hull, $6B$ on the ship side and $2L$ under the still water level. The air region extends approximately to $1L$ above the still water surface.

An arbitrary case of Froude number and trim angle is considered and the obtained solution is compared against the result of empirical formulas. A sample of computed free surface profile is illustrated in Figure 6 and comparison shows that numerical modeling has a reasonable agreement with the experimental study of Savitsky and Morabito [16].

6. Results

In this section, a prismatic planing hull with a 10 degree deadrise angle is investigated. The planing hull is examined in various conditions of Froude number and trim angle (Table 2). Likewise, the entire simulations

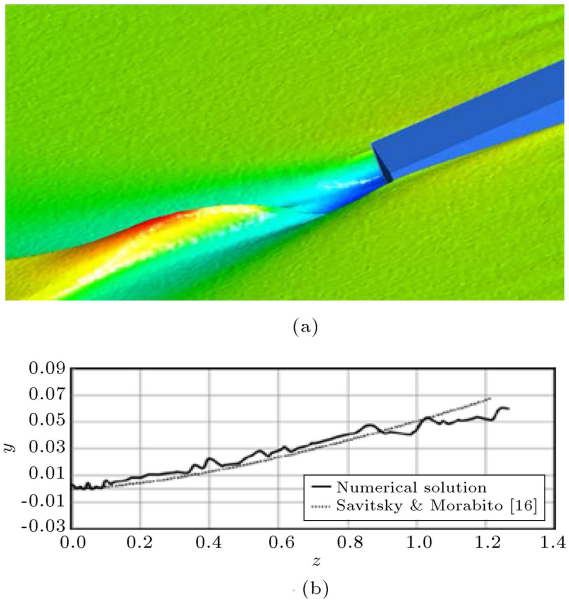

Figure 6. Validation of numerical computation of the transom stern flow: a) The obtained free surface; and b) the free surface elevation at center line.

Table 2. List of test cases.

		Trim			
		3	**6**	**9**	**12**
Fn	**1**	✓	✓	✓	✓
	2	✓	✓	✓	✓
	3	✓	✓	✓	✓

are repeated for the case of modified transom stern to study the effects of the reduction scheme in comparison with the full transom condition. Planning crafts commonly operate at Froude numbers above Fn = 1 and mostly under approximately Fn = 3. Therefore, the modified transom is tested in this range of Froude numbers. The length, width and height of the hull have been set equal to 2.0 m, 0.5 m and 0.3 m, respectively. A parametric study has been conducted on the trims and Froude numbers for $L_C = (1/12) * L = 0.167$ m, $H_C = 0.067$ m and $0 = 130$ deg (parameters defined in Figure 2).

In the following sections, the efficacy of the modified transom is assessed by the use of numerical analysis.

6.1. Froude number = 1.0

The free surface profile related to Fn = 1.0 is presented for various trim angles and the effect of modified transom stern is discussed. In Figure 7, the free surfaces are depicted at trim angle $\tau = 3$ and a comparison is made between the fully and modified transom stern waves. Also, the mesh used on the cut-away is illustrated in Figure 8.

It is noteworthy that since 3-D plots are not convenient for the analysis of the free surface profiles, the rooster tails are shown only along the centerline of the body for all the other considered cases. In Figure 9, the free surface contours corresponding to Fn = 1 at different trim angles are presented.

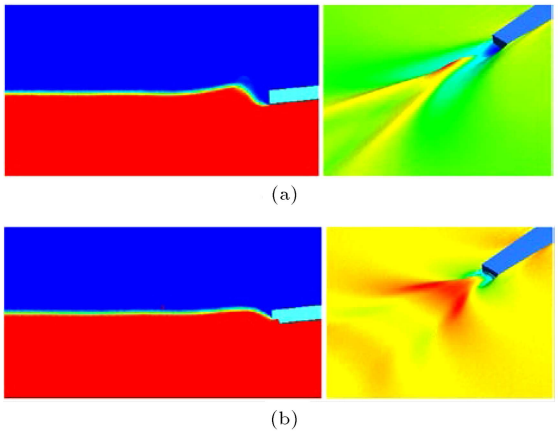

Figure 7. Free surface related to Fn = 1.0 and $\tau = 3$ for (a) full transom, and (b) modified transom 3-D pofiles of planing hull in motion are given on the hand sides of plots (a) and (b).

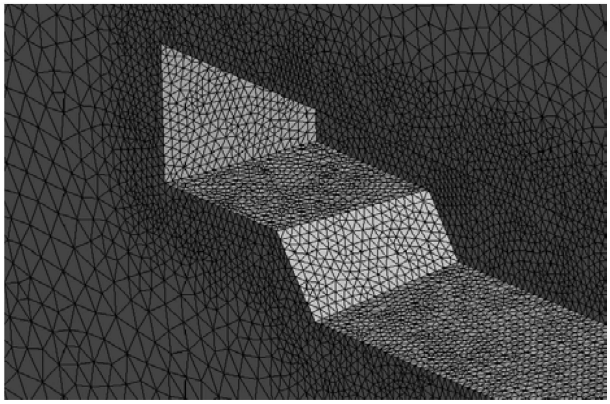

Figure 8. A close up view of the mesh used on the cut-away.

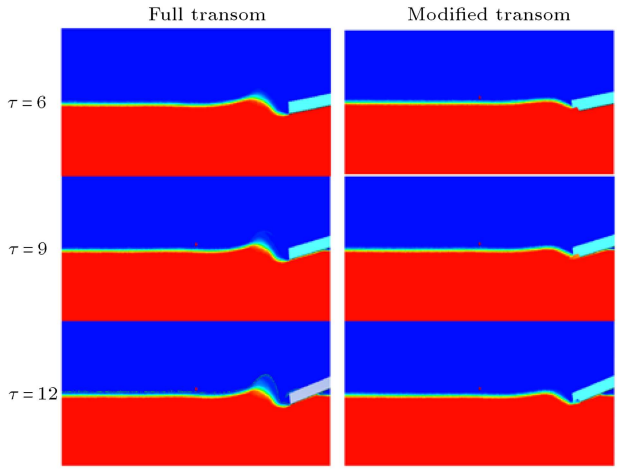

Figure 9. Free surface contours related to Fn=1.0.

The free surface profiles for the above cases are illustrated in Figure 10.

It is observed that at Fn = 1.0 and $\tau = 3$, ventilation process occurs and the transom is fully dried. The positive effect of the modified transom stern on the transom wave is also clearly observed in Figures 9 and 10. It is clear that the transom wave known as the "rooster tail" has been dramatically reduced. However, the longitudinal position of the wave crest is not changed.

The same observation is valid for other trim angles at Froude number 1. As a preliminary deduction, the rooster tail may strongly be reduced using the introduced transom shape. In fact, the wave height just behind the transom stern is decreased which may lead to a radar signature reduction. Furthermore, because of a reduction in wave making resistance, it may be easily deduced that the wave resistance and fuel consumption are also decreased.

It is also observed that at Fn = 1 and $\tau = 12$, the cut transom in contrast to the previous cases remains dry and the flow detaches from the keel. Although, this mechanism is not completely understood by the authors. It may indeed be due to the large trim angle.

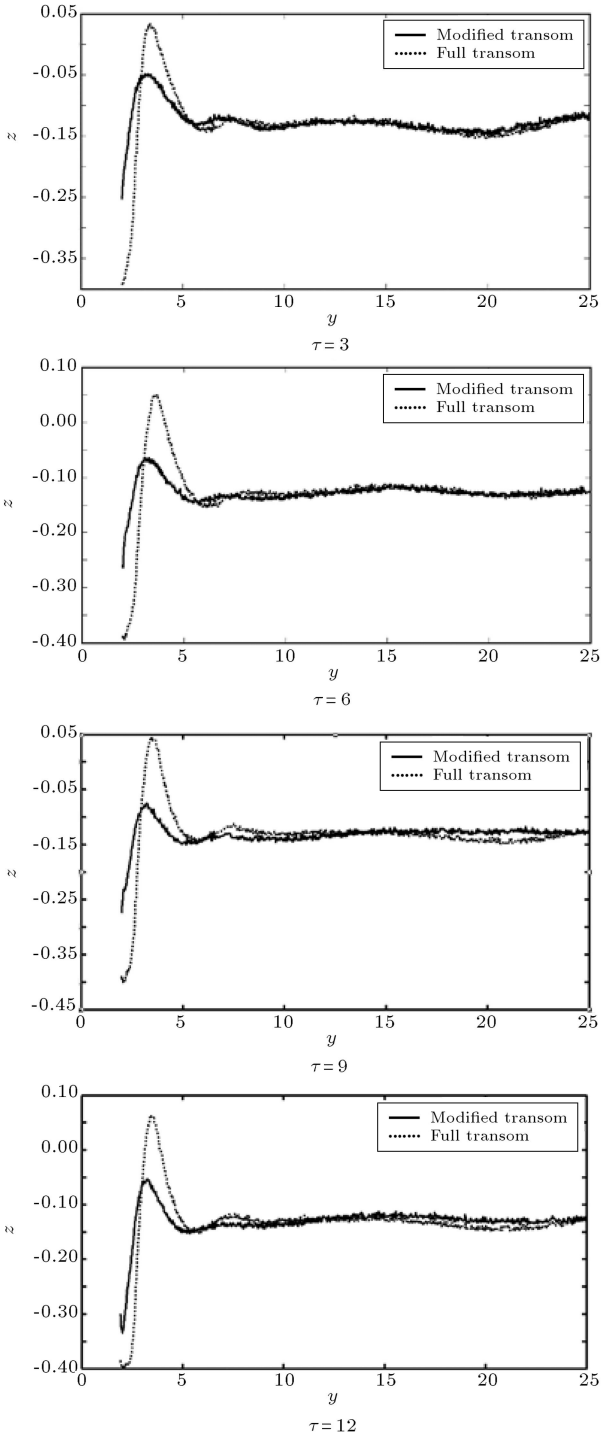

Figure 10. Comparison of the centerline free surface between full transom (- - -) and modified transom (—) at Fn = 1.0 at different trim angles.

6.2. Froude Number = 2.0

In the case of Fn = 2.0, the free surface flow can be different from Fn = 1.0. Therefore, presenting the obtained results and surveying the effect of the modified transom on the rooster tail at various trim angles can also be interesting.

Free surface profiles related to different trim angles at Fn = 2 are depicted in Figures 11 and 12.

It is observed that the modified transom stern not only has lightly increased the height of the rooster tail, but also has decreased its length. The reason behind what happens in this case will be discussed in the next section. However, it is clear that the reduction scheme has a reasonable positive effect on the rooster tail $\tau = 6$, as evidenced in Figure 12. Although, the

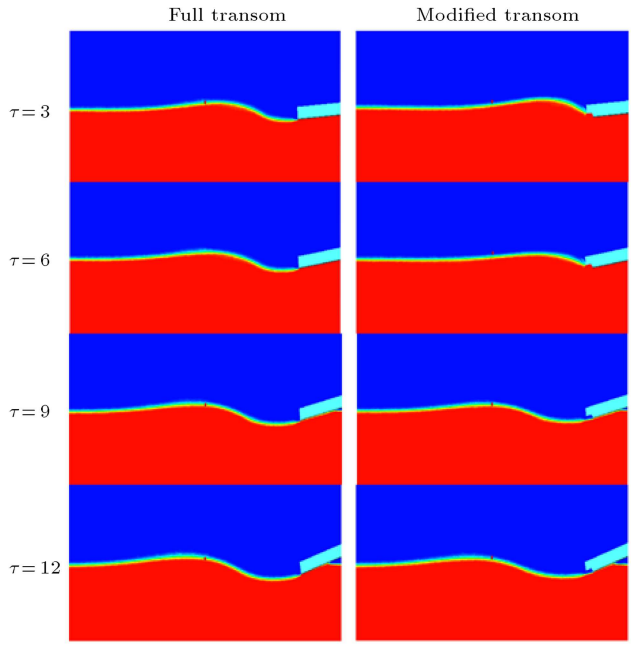

Figure 11. Free surfaces related to Fn = 2.0 at different trim angles.

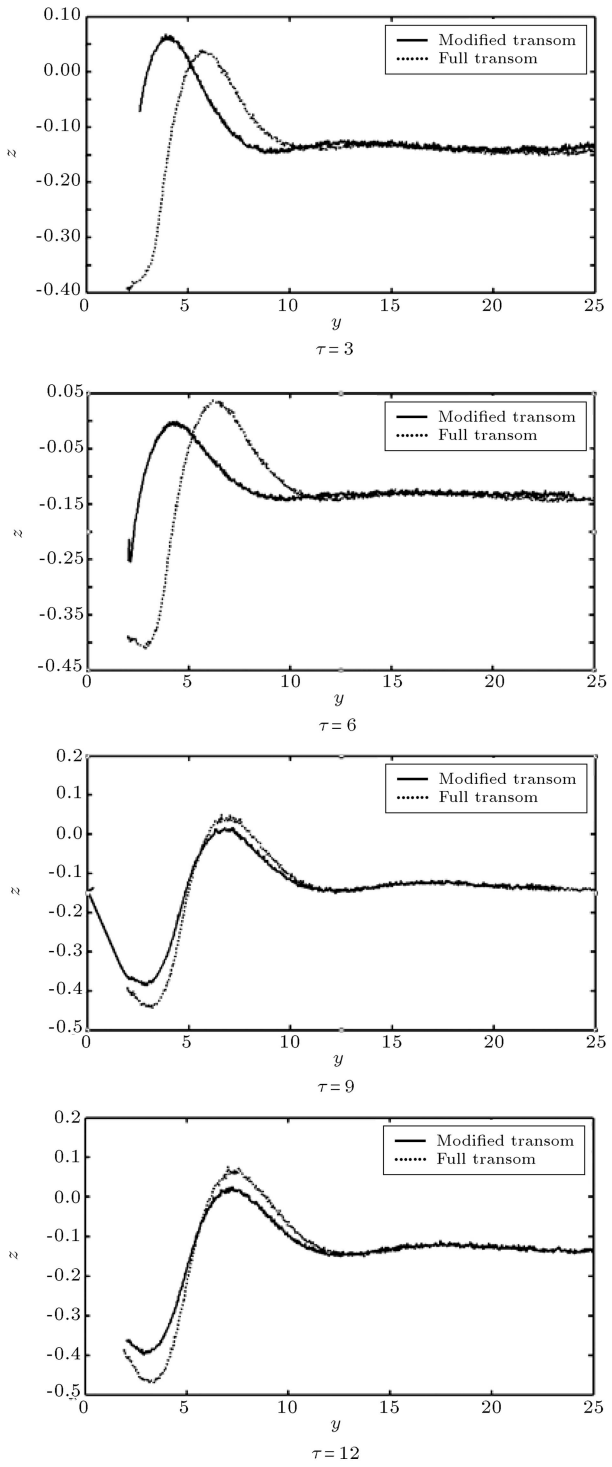

Figure 12. Comparison of the centerline free surface between full transom (- - -) and modified transom (—) at Fn = 2.0 at different trim angles.

modified transom could reduce the transom wave in this situation, the wave resistance may be increased due to an amplification of wave height near the hull. Albeit, it should be mentioned that the dramatic reduction in length of the rooster tail is a positive effect of the cutaway transom.

Also it is clear that using the suggested reduction scheme leads to the modification of the transom waves, and a desirable reduction in the wave amplitude may be achieved.

In the cases of trim angles 9 and 12 degrees and Fn = 2, a behavior similar to the case of Fn = 1 and trim angle 12 is observed, i.e. the flow separated from the keel and the lower part of the transom are dry.

6.3. Froude Number = 3.0

Study of the rooster tail characteristic, at very high speed condition which corresponds to Fn = 3.0, is very favorable for many researchers.

The free surface flow obtained from the three dimensional numerical computations for the cases τ = 3 to 12 are demonstrated in Figures 13 and 14.

The obtained results indicate that the modified transom has an undesirable performance for τ = 3 and 6 with regard to the height of the transom waves, but the length of the Rooster tail is dramatically reduced. However, the authors believe that by performing a series of parametric study on the geometric parameters of the cut, an optimum size of the suggested cut may be found to obtain the best performance. It is also observed in Figures 13 and 14 that the reduction scheme has positive effect on the transom stern wave related to the cases of τ = 9 and 12.

Based on Figure 14, it is seen that flow separation from keel occurs at Fn = 3 and τ = 9, 12. Therefore, it can be concluded that this phenomenon only happens when the trim angle is relatively high. In the next section, the overall effectiveness of the new transom is discussed.

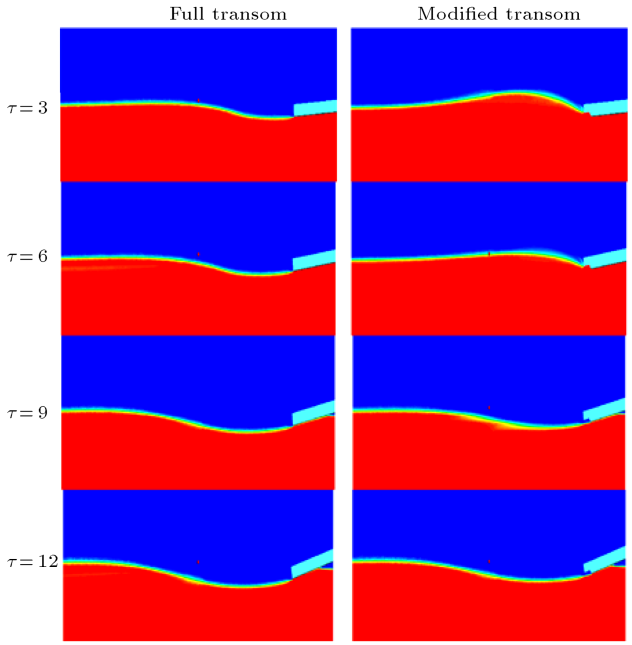

Figure 13. Free surface related to Fn = 3.0.

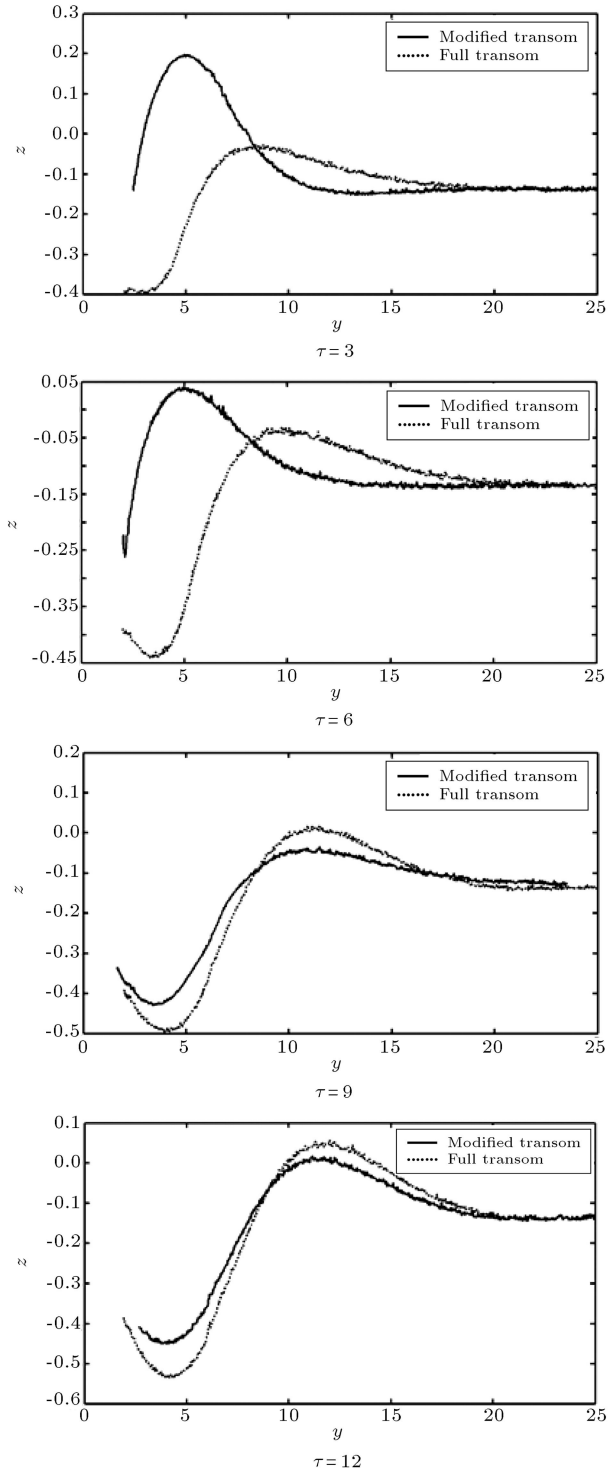

Figure 14. Comparison of the centerline free surface between full transom (- - -) and modified transom (—) at Fn = 3.0 at different trim angles.

7. Discussion of obtained results

In the last section, the obtained results for different trim angles and Froude numbers were illustrated, and it was qualitatively observed that the new transom form can reduce the rooster tail height and length.

Table 3. Rooster tail height and length reduction.

Fn	Trim	Length reduction (%)	Height reduction (%)
1	3	8.25%	44.70%
	6	13.63%	56.87%
	9	23.13%	61.79%
	12	15.63%	54.54%
2	3	37.50%	-6.82%
	6	49.35%	4.00%
	9	35.75%	16.86%
	12	1.00%	22.11%
3	3	53.33%	-49.35%
	6	63.07%	-21.50%
	9	5.79%	31.56%
	12	2.00%	18.55%

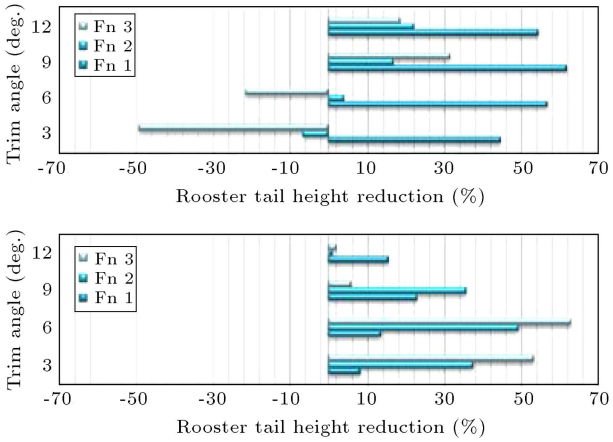

Figure 15. The effect of the new transom on the height and length of the rooster tail.

To quantify the values of the reduction in each case, Table 3 is provided.

The best performance of the introduced transom on the height reduction is gained at Fn = 1. By increasing the velocity (Fn), the performance of the new transom shape varies. At Fn = 2 and trim angle 3, wave crest significantly increases. At Fn = 3 and trim angles 3 and 6 degrees, similar behavior is also detected. However, the length of the rooster tail decreases significantly for all cases. The performance of the presented cutaway is better observed in the charts presented in Figure 15.

As clearly observed in Figure 15, the obtained results prove that the introduced transom shape has a dramatic positive effect in most cases.

The main question that we encounter here is: How the modified transom shape can lead to a rooster tail reduction? To address this question, the pressure variation in the transom stern region should be explored.

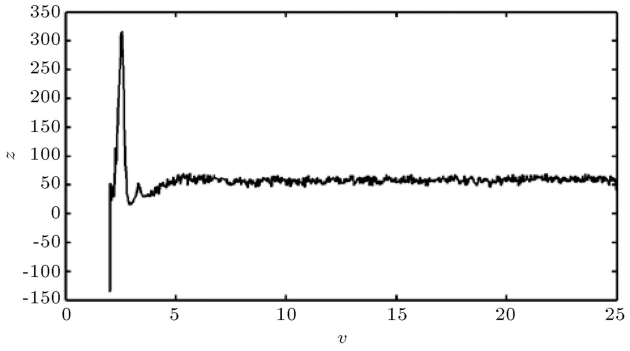

Figure 16. Pressure compression under the hull.

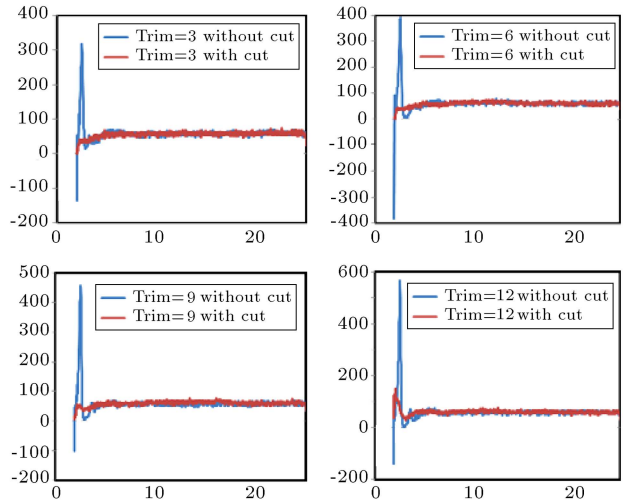

Figure 17. Pressure modification using the cutted transom stern at Fn = 1 and τ = 3, 6, 9 and 12 degrees.

Figure 16 shows that an intensive pressure variation exists in the lower edge of the transom stern. Based on this observation, it can be stated that, as the pressure of the water under the hull experiences an abrupt change, water rapidly moves upwards, immediately behind the transom. Therefore, to reduce the stern wave, an abrupt pressure variation must be modified.

The above explanations may look very superficial at a first glance, but the modification of the intensive pressure variations by the introduced transom form which is observed in Figures 17 through 19, for different case studies, can very well support the offered reasoning.

The pressure modification after implementing the cutted transom is illustrated in Figure 17. It is observed that the intensive pressure variation is corrected in all cases. Therefore, the generated rooster tail is also modified, effectively.

While the pressure variation and consequently the rooster tail are modified, using the cut transom, there still exist some cases where no appealing results on the rooster tail height are achieved. For example, at Fn = 2 for the trim angle 3 degrees, and Fn = 3 for the trim angles of 3 and 6 degrees, the increases in rooster

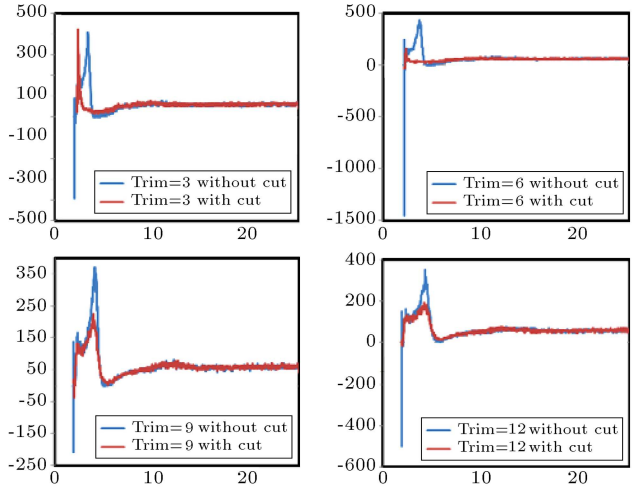

Figure 18. Pressure modification using the cutted transom stern at Fn = 2 and τ = 3, 6, 9 and 12 degrees.

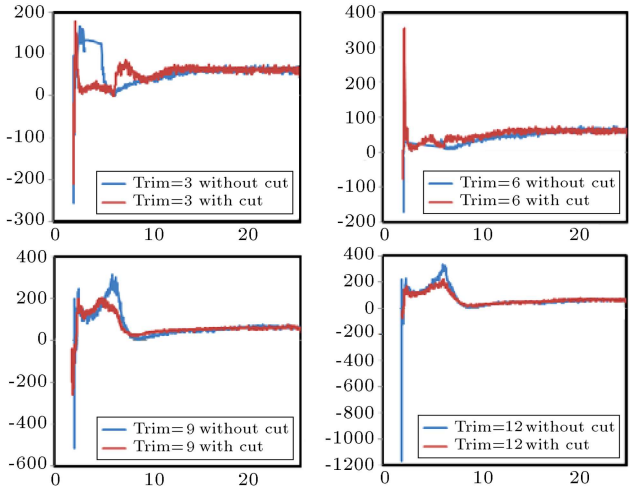

Figure 19. Pressure modification using the cutted transom stern at Fn = 3 and τ = 3, 6, 9 and 12 degrees.

tail height are observed. However, when the height increases, the length of the rooster tail is dramatically reduced which may lead us to conclude that the positive pressure variation control has affected the length of the rooster tail.

Figure 18 shows that the pressure variation becomes larger at Fn = 2 for the trim angle 3 degrees. In the meantime, at the trim angle 3 degrees, the free surface profile intensifies which was previously illustrated in Figures 18 and 19. However, at other considered trim angles, modification of pressure variation is also proved to be effective which are depicted in Figure 18.

The influence of the cut transom on pressure variation at Fn = 3, is completely analogous to the previous case of Fn = 2, except for the trim angle 6 degrees (Figure 19). For the trim angles 3 and 6 degrees, the pressure variation is intensified, and consequently stronger rooster tail is formed, which was observed in Figure 14. At two other trim angles,

desirable pressure modification and wave reduction are achieved.

Based on the results presented in Figures 17 through 19, one can conclude that in order to reduce the transom stern wave height, the intensive pressure variation must be modified, and this point should be considered as a design point which might be a very interesting deduction. Furthermore, one also has to be mindful of the fact that optimum dimensions of the cut should be indeed based on the operational limitations of the considered planing craft. It is due to this fact that operational benefits of an introduced transom form may be affected by the hull form and the flow condition.

8. Conclusion

A modified transom stern shape is presented and by using a three dimensional numerical computation, effect of this modification on the transom stern wave, known as "rooster tail", is probed. In fact, modification of rooster tail waves leads to a radar signature reduction. In this context, by using Ansys-CFX software, Finite Volume Method (FVM) in conjunction with Volume Of Fluid (VOF) scheme is utilized to explore the effect of the suggested reduction scheme on the 3D transom wave, numerically. Mesh convergence study is presented for a wide range of element size and it is also verified that the numerical model has a good accuracy in comparison with the empirical formula of Savitsky.

A set of Froude numbers including 1.0, 2.0 and 3.0, and trim angles consisting of 3, 6, 9 and 12 degrees, have been considered to perform a parametric study and survey on the effects of the introduced transom shape.

It has been observed that the transom wave height is reduced in many cases by using the presented reduction idea. However, in the case of Froude numbers 2 and 3 and trim angle 3, the transom stern modification leads to an increase in the wave height and the rooster tail may be intensified. But the length of the rooster tail is effectively decreased in all cases. The reasons for the wave reduction have been discussed and it is concluded that the transom stern modification can show a way by which the pressure underneath the transom stern exhibits minimum variation, which in turn causes a reduction in the height of the rooster tail.

Based on the presented results, it is observed that the performance of the cut transom on the rooster tail reduction is very much affected by the flow condition. Consequently, in order to have the best performance in the rooster tail reduction, it is necessary to perform systematic computations for the cut dimension selection. In this paper, the authors intended to numerically demonstrate how it is possible to reduce the transom stern waves by the cut transom for a particular hull shape and offer a set of parametric studies to show the effects of Froude numbers and the trim angles in the process. Performing a huge parametric study on different planing hull forms is beyond the scope of this paper and was not targeted, here.

Additionally, the main contribution of the present article can be categorized as follows:

- Three dimensional viscous numerical solution of the transom stern flow;
- Proving (by use of numerical computation) that an innovative transom form can reduce stern the wave;
- Conducting a wide range of parametric studies on Froud numbers and trim angles;
- Finding how the reduction of the rooster tail can be affected by correcting the pressure change as a design point.

Obviously, the particular shape of any hull and the applied flow condition would require its own investigation. Therefore, to make use of the introduced transom form, researchers must naturally conduct their own parametric studies on the prevailing flow condition for their desired hull. Computations related to the performance of the cutted transom in regular and irregular waves will be conducted in future works. Furthermore, determination of propeller effect on the rooster tail reduction scheme can be considered as a very exciting study.

References

1. Karafiath, G. and Fisher, S.C. "The effect of stern wedges on ship powering performance", *Nav. Engs. J.*, **3**, pp. 27-38 (1987).
2. Cusanelli, D. and O'Connell, L. "U.S. coast guard island class 110 wpb: Stern flap evaluation and selection (Model 5526)", Report, Carderock Division, Naval Surface Warfare Center, Hydromechanics Department (1999).
3. Karafiath, G. "Hydrodynamic efficiency improvement to the USCG 110Ft WPB ISLAND class patrol boat", *SNAME Transactions*, **109**, pp. 197-220 (2001).
4. Salas, M., Rosas, J. and Luco, R. "Hydrodynamic analysis of the performance of stern flaps in a semi-displacement hull", *Latin American Appl. Res.*, **34**, pp. 275-284 (2004).
5. Yamano, T., Kusunoki, Y., Kuratani, F., Ogawa, T., Ikebuchi, T. and Funeno, I. "Effect of transom stern bottom profile form on stern wave resistance-An experimental study", *J. Kansai. Soc. N. A. Japan*, **239**, pp. 1-10 (2003).
6. Yamano, T., Kusunoki, Y., Kuratani, F., Ogawa, T., Ikebuchi, T. and Funeno, I. "Effect of transom stern

bottom profile form on stern wave resistance- A consideration on the effect of real stern end immersion", *J. Kansai. Soc. N. A. Japan*, **240**, pp. 11-19 (2003).

7. Ogilat, O., McCue, S.W., Turner, I.W., Belward, J.A. and Binder, B.J. "Minimising wave drag for free surface flow past a two-dimensional stern", *Phys. Fluids*, **23**, pp. 72-101 (2011).

8. Robards, S. and Doctors, L.J. "Transom-hollow prediction for high-speed displacement vessels", *Proc. of Intl. Conf. on Fast Sea Transp. (FAST '03)*, **7**, Ischia, Italy, 1, pp. A1.19-A1.26 (2003).

9. Doctors, J. "Hydrodynamic of the flow behind a transom stern", *Proc. of the Conf. on Mech. Engrg.*, **29**, Haifa (2003).

10. Doctors, J. "Influence of the transom-hollow length on wave resistance", *Proc. 21st Intl. Workshop on Water Waves and Floating Bodies (21 IWWWFB)*, Loughborough, England (2006).

11. Maki, J.K., Doctors, J.L., Beck, R. and Troesch, A. "Transom-stern flow for high-speed craft", *Intl. Conf. on Fast Sea Transp.*, **8**, Saint Petersburg, Russia, pp. 191-199 (2005).

12. Doctors, J.L. and Beck, R. "The separation of the flow past a transom stern", *Proc. of the Intl. Conf. on Marine Research and Transp.*, **1**, Ischia, Italy (2005).

13. Maki, J.K., Troesch, A. and Beck, R. "Qualitative investigation of transom stern flow ventilation", *Proc. of Intl. Workshop on Water Waves and Floating Bodies*, **19**, Cortona, Italy, pp. 28-31 (2005).

14. Fu, T., Fullerton, A., Ratcliffe, T., Minnick, L., Walker, D., Lee Pence, M. and Anderson, K. "A detailed study of transom breaking waves", Report, Carderock Division, Naval Surface Warfare Center, Hydromechanics Department (2009).

15. Fu, T., Fullerton, A., Drazen, D., Minnick, L., Walker, D., Ratcliffe, T., Russell, L. and Capitain, M. "A detailed study of transom breaking waves: Part II", Report, Carderock Division, Naval Surface Warfare Center, Hydromechanics Department (2010).

16. Savitsky, D. and Morabito, M. "Surface wave contours associated with the forebody wake of stepped planing hulls", *Meeting of the NY Metropolitan Section of the Soc. of Nav. Architects and Marine Engineers* (2009).

17. Haussling, H. "Two dimensional linear and nonlinear stern waves", *J. Fluid Mech.*, **97**, pp. 759-769 (1980).

18. Cheng, B. "Computations of 3D transom stern flows", *Proc. of Intl. Conf. on Numerical Ship Hydrodynamics*, **5**, Washington DC, USA, pp. 581-592 (1989).

19. Scorpio, S. and Beck, R.F. "Two-dimensional inviscid transom stern flow", *Proc. of Intl. Workshop on Water Waves and Floating Bodies*, **12**, Carry-le-Rouet, France, pp. 221-226 (1997).

20. Sireli, E.M., Insel, M. and Goren, O. "The effects of transom stern on the resistance of high speed craft", *IMAM*, Naples, pp. 40-47 (2000).

21. Binder, B.J. "Steady free surface flow at the stern of a ship", *J. Physics of Fluids*, **22**, 012104, 5 pages (2010).

22. Haussling, H.J., Miller, R.W. and Coleman, R.M. "Computation of high speed turbulent flow about a ship model with a transom stern", Report, Carderock Division, Naval Surface Warfare Center, Hydromechanics Department (1997).

23. Schweighofer, J. "Investigation of two-dimensional transom waves using inviscid and viscous free-surface boundary conditions at model- and full-scale ship Reynolds numbers", *5th Numerical Towing Tank Symp.* (2002).

24. Starke, B., Ravan, H. and Van Der Ploeg, A. "Computation of transom-stern flows using a steady free-surface fitting RANS method", *Intl. Conf. on Numerical Ship Hydrodynamics*, **9**, Michigan (2007).

25. Maki, K.J., Iafrati, A., Rhee, S., Beck, R. and Troesch, A. "The transom-stern modeled as a backward facing step", *Symp. on Nav. Hyd.*, **26**, Rome, Italy, pp. 17-22 (2006).

26. Maki, K.J., *Transom Stern Hydrodynamics*, Doctoral Thesis, University of Michigan (2006).

27. Ferziger, J.H. and Perić, M., *Computational Methods for Fluid Dynamics*, Springer, 3rd Edn. (2002).

28. Pope S.B., *Turbulent Flows*, Cambridge University Press (2000).

Biographies

Parviz Ghadimi received his PhD degree in Mechanical Engineering in 1994 from Duke University, USA. He served one year as a Research Assistant Professor in M.E. and six years as a Visiting Assistant Professor in Mathematics Department at Duke. He is currently an Associate Professor of Hydromechanics in Department of Marine Technology at Amirkabir University of Technology, Iran. His main research interests include hydrodynamics, hydro-acoustics, thermo-hydrodynamics, and CFD and he has authored several scientific papers in these fields.

Abbas Dashtimanesh received his PhD degree in Hydromechanics from Department of Marin Technology at Amirkabir University of Technology in 2013. He is currently an assistant professor at Persian Gulf University. His main research interests include numerical methods in hydromechanics, designing and hydrodynamic of planing hulls and dynamics of marine vehicles.

Rahim Zamanian received his PhD degree in Mechanical Engineering in 2003 from Iowa State Univer-

sity, USA. He is currently an Assistant Professor in Mechanical Engineering Group of International Branch at Amirkabir University of Technology, Iran. His main research interests include Continuum Mechanics, Vibrations, and Hydro-elasticity, and he has authored several scientific papers in these areas.

Mohammad A. Feizi Chekab received his Bachelor of Science and Master of Science degrees in Marine Engineering and Naval Architecture from Amirkabir University of Technology in years 2006 and 2009, respectively. He was then admitted to the PhD program to the Department of Marine Technology in year 2010 and is currently working on his dissertation. His main research interests include hydrodynamics and hydroacoustics and he has authored many articles on these topics.

Seyed Hamid R. Mirhosseini finished his Bachelor of Science degree in Marine Engineering at Amirkabir University of Technology in year 2008. He was then admitted to the Master of Science program in Ship Hydrodynamics at Amirkabir University of Technology where he received his MSc degree in year 2012. He has authored three papers in the area of ship hydrodynamics.